

Late Holocene changes in vegetation and atmospheric circulation at Lake Uddelermeer (The Netherlands) reconstructed using lipid biomarkers and compound-specific δD analysis

V. VAN DEN BOS,^{1,2*} S. ENGELS,^{1,3} S. J. P. BOHNCKE,^{4,†} C. CERLI,¹ B. JANSEN,¹ K. KALBITZ,^{1,5} F. PETERSE,⁶ H. RENNSSEN^{4,7} and D. SACHSE⁸

¹Institute for Biodiversity and Ecosystem Dynamics, University of Amsterdam, Amsterdam, The Netherlands

²School of Geography, Environment and Earth Sciences, Victoria University of Wellington, Wellington, New Zealand

³Centre for Environmental Geochemistry, School of Geography, University of Nottingham, Nottingham, UK

⁴Department of Earth Sciences, Section Climate Change & Landscape Dynamics, VU University Amsterdam, Amsterdam, The Netherlands

⁵Institute of Soil Science and Site Ecology, Dresden University of Technology, Tharandt, Germany

⁶Department of Earth Sciences, Utrecht University, Utrecht, The Netherlands

⁷Department of Natural Sciences and Environmental Health, University College of Southeast Norway, Bø i Telemark, Norway

⁸Helmholtz Centre Potsdam, GFZ German Research Centre for Geosciences, Section 5.1 Geomorphology, Potsdam, Germany

Received 23 February 2016; Revised 25 June 2017; Accepted 27 September 2017

ABSTRACT: We reconstructed middle to late Holocene changes in atmospheric circulation patterns and vegetation in north-west Europe by applying novel geochemical techniques to the sediment record of Lake Uddelermeer (The Netherlands). A comparison of higher plant-derived leaf wax *n*-alkane distributions archived in the lake sediments with those in living plant material, combined with palynological analysis, indicates that the vegetation immediately surrounding the lake became more open at 3150 cal a BP, while the regional vegetation responded more gradually and ~650 years later. Our record of the hydrogen isotopic composition of plant leaf waxes (δD_{wax}) shows a deuterium enrichment starting from 3500 cal a BP, which we interpret as a change in atmospheric circulation. A similar δD_{wax} record from nearby Meerfelder Maar (Germany) shows an opposite trend around this time, which could be explained by a change in sea-level pressure resembling a negative North Atlantic Oscillation phase. This could account for depleted δD values of precipitation at Meerfelder Maar, while confounding factors related to the more maritime position of Uddelermeer cause the opposite shift there. Copyright © 2018 John Wiley & Sons, Ltd.

KEYWORDS: atmospheric circulation; compound-specific δD analysis; lipid biomarkers; North Atlantic Oscillation; north-west Europe.

Introduction

Holocene climate in the Northern Hemisphere is characterized by several distinct climatic events, some of which have been correlated to variations in solar output (e.g. the so-called 2.8-kyr event and the Little Ice Age; Mauquoy *et al.*, 2002; van Geel *et al.*, 2014). These events have been identified in lake sediment parameters (Haltia-Hovi *et al.*, 2007; Martin-Puertas *et al.*, 2012; Ojala *et al.*, 2015; Czymzik *et al.*, 2016), peat bogs (e.g. van Geel *et al.*, 1996, 2014), and other terrestrial and marine records (e.g. Bond *et al.*, 1997; Charman, 2010). The forcing mechanism that links climate and solar activity is poorly understood, but a role for drift ice variations related to ocean circulation (Bond *et al.*, 2001; Charman, 2010) and/or atmospheric circulation changes (e.g. Magny, 2004; Martin-Puertas *et al.*, 2012; Czymzik *et al.*, 2016) have been proposed. The current mode of atmospheric circulation responsible for climate variations in western Europe is the North Atlantic Oscillation (NAO; Olsen *et al.*, 2012), which controls the strength of the westerly winds and the location of storm tracks across the North Atlantic.

The 2.8-kyr event (van Geel *et al.*, 1996) is associated with the Subboreal–Subatlantic biozone transition identified in palynological records as a sudden decline in *Corylus avellana*

pollen, consistent with a transition to wetter and cooler climate conditions (e.g. van Geel, 1978; van Geel *et al.*, 1996). This transition is widespread and dominant in climate records of north-west Europe (e.g. Kilian *et al.*, 1995; Charman *et al.*, 2006; Swindles *et al.*, 2013; van Geel *et al.*, 2014; Engels *et al.*, 2016; Rach *et al.*, 2017). However, Mayewski *et al.* (2004) describe variable climate conditions from multiple locations around the world in an extended interval (3500–2500 cal a BP), indicating that the 2.8-kyr event might not constitute a uniform shift in climate. Indeed, a reconstruction of past hydrological changes at Lake Uddelermeer (The Netherlands; Fig. 1A) showed lake levels were approximately 2.5 m lower than present between 3150 and 2800 cal a BP, followed by a period of higher-than-present lake levels from 2800 cal a BP onward (Engels *et al.*, 2016). The inference of a lake-level lowstand just before the 2.8-kyr event is not in line with results derived from high-resolution reconstructions of past precipitation derived from nearby peat bogs, such as Engbertsdijksveen (Fig. 1A; van Geel *et al.*, 1996).

To better understand the environmental and climatic changes that occurred around the 2.8-kyr event at Lake Uddelermeer, we combine the data from leaf wax lipids (*n*-alkanes), their hydrogen-isotopic composition and branched glycerol dialkyl glycerol tetraethers (brGDGTs) from the same core, and compare them to the palynological record of Engels *et al.* (2016). Our record spans 6330–1500 cal a BP, covering

*Correspondence: V. van den Bos, ²School of Geography, as above.

E-mail: valerie.vandenbos@vuw.ac.nz

†Deceased.

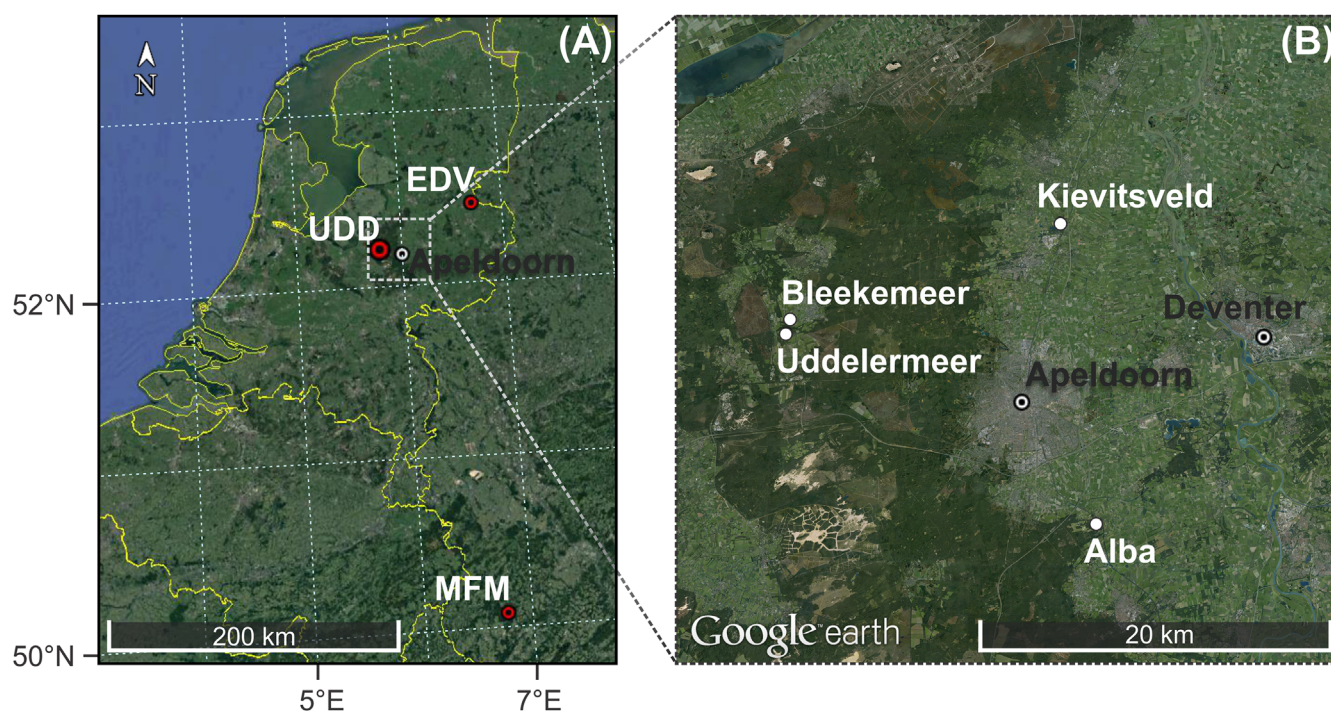


Figure 1. (A) Map of The Netherlands and parts of surrounding countries showing the location of our study site Lake Uddelermeer (UDD) and two sites mentioned in the text: Engbertsdijkveen (EDV) and Meerfelder Maar (MFM). (B) Enlarged map of the area around Lake Uddelermeer and the location of three other lakes where modern plant material was collected.

part of the middle Holocene (8200–4200 cal a BP) and late Holocene (4200 cal a BP to present; Walker *et al.*, 2012). The *n*-alkanes derived from the leaf wax of higher plants can be traced back to their source organism and can be used to distinguish local from regional vegetation changes when combined with palynological data (Eglinton and Eglinton, 2008). In addition, the hydrogen isotopic composition of these *n*-alkanes can be linked to hydrological changes in their source area (Sachse *et al.*, 2012). Finally, variations in the molecular composition of brGDGTs (membrane lipids produced by certain soil bacteria) can be used to reconstruct annual mean air temperatures (MATs) for the area in which they are produced (Weijers *et al.*, 2007).

Materials and methods

Site description

Lake Uddelermeer (52°14'48"N, 5°45'40"E) currently measures 300 m by 200 m and has a maximum water depth of 1.3 m. The lake is a focal point for groundwater flow as it is situated between two push moraines of Saalian age at an elevation of 24 m a.s.l. A pingo developed during the Last Glacial Maximum, which melted during the Weichselian Lateglacial ca. 14 000 years ago (Engels *et al.*, 2016). The lake formed in the resulting depression after the melting of the ice-lens, and lacustrine sediments started to accumulate, which have a maximum thickness of 15.6 m today. The lake is surrounded by a small fringe of wetlands (with willow *Salix cinerea* and birch *Betula pendula*) and bordered by a stand of trees on the west side (alder *Alnus glutinosa*). On the eastern side of the lake, a human-made defensive structure supports some oaks (*Quercus robur*), beeches (*Fagus sylvatica*) and pine trees (*Pinus sylvestris*). The bank and the surroundings of the lake have been inhabited since the Early Neolithic (Polak, 1959). The Netherlands currently experiences a maritime climate,

caused by prevailing south-westerly winds, which are a primary source of precipitation throughout the year. MATs lie around 10.1 °C (average over 1981–2010).

Sample collection

Collection of modern plant material

Plant leaves were collected for *n*-alkane and stable isotope measurements during fieldwork in April and May 2012. Plant species expected to be responsible for the dominant biomass input into the sediments of Uddelermeer were selected based on the pollen record and the present vegetation around the lake. Living leaf tissue was collected for these species (Table 1) in the immediate surroundings of Uddelermeer where possible. Species that were not present at Uddelermeer were collected at other lakes in the area (Fig. 1). As no significant biomass input from roots is expected in lacustrine sediment, only samples of leaves

Table 1. Plant species analysed for their *n*-alkane patterns, common names and location of collection (Fig. 1).

Scientific name	Common name	Location
<i>Alnus glutinosa</i>	Black alder	Bleekemeer
<i>Betula pendula</i>	Silver birch	Uddelermeer
<i>Corylus avellana</i>	Common hazel	Uddelermeer
<i>Fagus sylvatica</i>	Common beech	Uddelermeer
<i>Quercus robur</i>	English oak	Uddelermeer
<i>Salix cinerea</i>	Grey willow	Uddelermeer
<i>Tilia</i> sp.*	Lime	Uddelermeer
<i>Calluna vulgaris</i>	Common heather	Alba
<i>Phragmites australis</i>	Common reed	Uddelermeer
<i>Nuphar lutea</i>	Yellow water lily	Kievitsveld

*Not identified to species level; probably the naturally occurring hybrid *Tilia* × *europaea*, common lime.

were taken from each of the 10 species included in this study. Material was sampled from one to five specimens of the same species and mixed for analysis to obtain an average lipid signal (Jansen *et al.*, 2006). Hand contact with the samples was avoided during sampling to avoid lipid contamination and the samples were immediately wrapped in aluminium foil upon collection. The samples were freeze-dried and ground upon return to the laboratory.

Sediment coring and sample selection

The sediment core used in the present study is core UDD-E, which is one in a series of core sequences taken (in April and May 2012) at different positions along a north–south transect across the lake. The core was retrieved from the deepest part of the sediment basin (52°14′47.5″N, 5°45′39.5″E) using a 3-m-long UWITEC piston core deployed from a floating platform (Engels *et al.*, 2016). The sediment cores were stored in a cold room before processing. Core UDD-E has a length of ~14 m (1440–67 cm depth) and the present study focuses on the depth interval from 955 to 315 cm. The sequence consists of dark-brown algal gyttja with only a few visible macro-remains (mostly mosses).

A total of 59 3-cm-thick sub-samples were taken from the core for biomarker analysis at 10-cm intervals. As with the modern plant material, hand contact was avoided during sample treatment and the samples were freeze-dried and ground with a mortar and pestle. All samples were stored in clean glass vials until extraction. Samples for loss-on-ignition (LOI) and pollen analysis were taken from the same depths (middle cm).

Chronology

All data derived from the core sequence were plotted on a timescale based on the age–depth model for the entire core as published by Engels *et al.* (2016). The model is based on 26 ²¹⁰Pb measurements from the upper 66 cm of the sediments and 20 accelerator mass spectrometry (AMS) ¹⁴C samples distributed through the core, combined using Bayesian modelling as included in the OxCal software (Bronk Ramsey, 2009). The core interval analysed in this study ranged from 955 to 315 cm depth, equivalent to 6330–1500 cal a_{BP}, thus including the 2.8-kyr event. The age–depth model shows relatively well-constrained age estimates for the period 3000 cal a_{BP} to the present (average uncertainty of ±150 years based on 2-sigma error estimates). The 2-sigma error on age estimates is larger in the lower part (average uncertainty of ±400 years) due to the low content of material (macro-remains) suitable for radiocarbon dating. The age–depth model should therefore be treated with caution for the age interval 6330–3000 cal a_{BP} (Engels *et al.*, 2016).

Palynology and loss-on-ignition

Engels *et al.* (2016) presented a pollen diagram for the entire UDD-E core, and compared their results against a pollen record retrieved from the littoral of the lake to identify hiatuses. Here, we re-interpret the data from Engels *et al.* (2016) for the 6330–1500 cal a_{BP} interval in the context of vegetation development and changes of the terrestrial and aquatic ecosystems. A pollen percentage diagram for 6330–1500 cal a_{BP} was replotted (using the Rioja package in R 3.1.2; R Core Team, 2014; Juggins, 2015). LOI data from Engels *et al.* (2016) were plotted as well to aid with interpretation. Zonation was determined by Engels *et al.* (2016), following the Blytt–Sernander scheme.

Biomarker analysis

A more detailed description of the methods used to analyse biomarkers is provided as Supporting Information (Appendix S1).

Before lipid extraction, the carbon, nitrogen and sulphur content was measured using ~5 mg of each sediment sample. The C/N ratio was calculated from the carbon (C) and nitrogen (N) concentrations. Approximately 0.1–0.2 g of each of the leaf samples and 1-g sediment sub-samples were processed to extract the lipids. Thereafter the extracts were separated into several fractions based on polarity (Sachse *et al.*, 2004). The aliphatic fraction, containing the *n*-alkanes, was analysed by gas chromatography-mass spectrometry (GC/MS). The ratios of *n*-alkanes of various chain lengths within the extract from the sediment samples were investigated and compared to the lipid patterns in the plant species to enable a reconstruction of past vegetation changes.

Compound-specific hydrogen isotope ratios (expressed as a δD value) of the *n*-alkanes were subsequently measured on an isotope ratio mass spectrometer. Three replicate measurements were performed on each sample. All δD values were normalized to the Vienna Standard Mean Ocean Water (VSMOW) scale using a linear regression function between measured and certified δD values of a standard mix.

The alcohol/fatty acid fraction of the lipid extracts, containing the GDGTs, was analysed according to the latest chromatography method with improved separation of GDGT isomers (cf. Hopmans *et al.*, 2016), using *ultra* high-performance liquid chromatography/atmospheric pressure chemical ionization-mass spectrometry (HPLC/APCI-MS).

All biomarker data were plotted in R 3.1.2 (R Core Team, 2014) using package ‘ggplot2’ (Wickham, 2009).

Results

Modern leaf material

The *n*-alkane composition of the leaf extracts from the ten selected plant species (Table 1) is presented in Fig. 2. The *n*-alkane patterns comprise homologues in the chain length range C₂₃–C₃₃, with a strong odd-over-even preference. Most species are characterized by a unique *n*-alkane pattern. For instance, *Calluna vulgaris*, a common species of heathland and some bog types, contains high concentrations of C₃₃, a chain length not commonly observed in the other taxa. Second, the number of major homologues present differs substantially between the individual species: e.g. *Fagus sylvatica* shows only one major *n*-alkane peak (C₂₇), whereas *Quercus robur* shows high concentrations of four chain-length homologues. Some species, however, show very similar *n*-alkane distributions, such as *Alnus glutinosa* and *Salix cinerea*, which produce C₂₇ and C₂₉ in similar concentrations. *Tilia* sp. and *Corylus avellana* both show a high peak at C₂₉ and a secondary dominant abundance of C₃₁. Tree species *Betula pendula* produces both mid-length chains (C₂₃ and C₂₅) and longer chains (C₂₇, C₂₉ and C₃₁). The distribution of grass species *Phragmites australis* is dominated by C₂₉. The only analysed aquatic species, *Nuphar lutea*, contains *n*-alkane homologues in the same range as the terrestrial species, with dominant contributions of C₂₇ and C₂₉.

There are large differences in *n*-alkane concentrations between the different plant species. The concentration of the most abundant homologues in *A. glutinosa*, *B. pendula*, *F. sylvatica*, *S. cinerea* and *C. vulgaris* exceeds 100 μg g⁻¹ dry leaf material. The major *n*-alkane homologue in *Tilia* sp. reaches 30 μg g⁻¹, while the other species contain concentrations of around 10 μg g⁻¹ per homologue or less. The

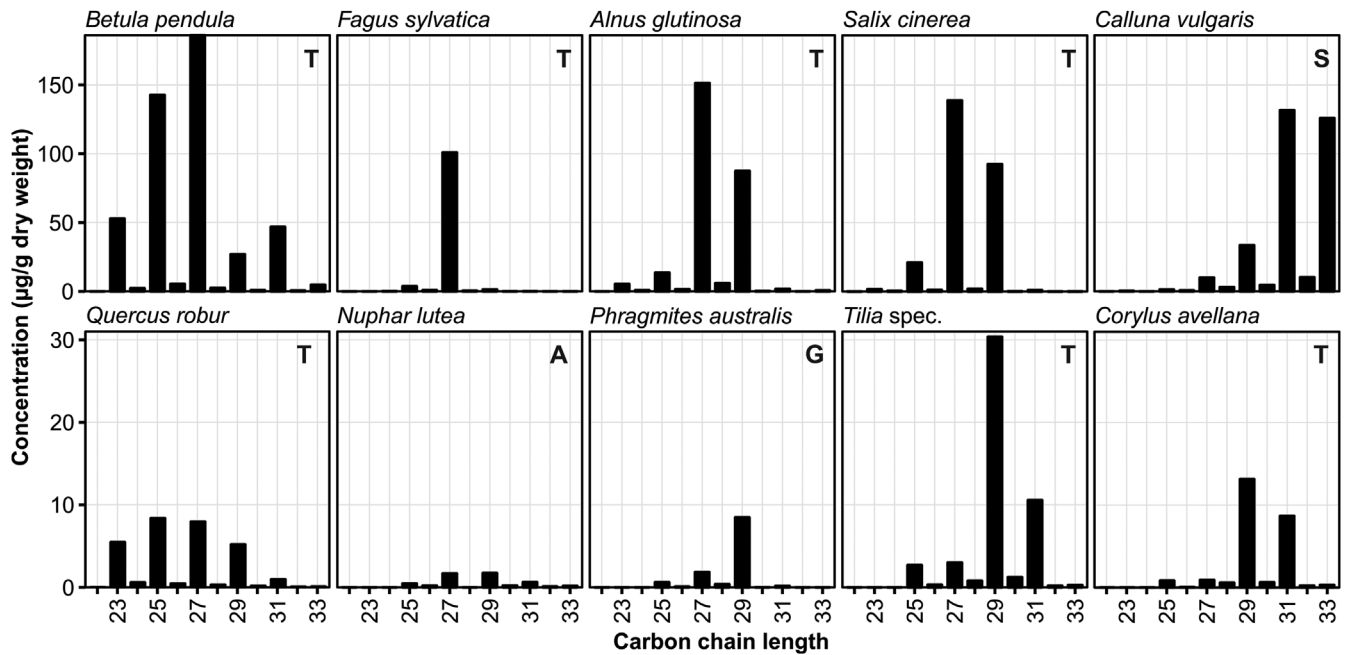


Figure 2. Distribution of *n*-alkanes extracted from the modern material (leaves) of 10 plant species. The plant type is indicated in the right-hand corner of each graph (A=aquatic, G=grass, S=shrub, T=tree). Note that the y-axis is differently scaled for each row. Common names of the plant species and collection sites can be found in Table 1.

homologues of *N. lutea* do not exceed $2 \mu\text{g g}^{-1}$ dry leaf material.

Holocene sediment record

Palynological data and C/N ratio

A selection of taxa from the pollen percentage diagram is presented in Fig. 3. Our record includes part of the Atlantic, the Subboreal and part of the Subatlantic biozone. The main contributors of arboreal pollen are *Alnus* and *Quercus*, while *Betula* and *Corylus avellana* are also present in relatively high

abundances (Fig. 3). The percentage of arboreal pollen decreases gradually through time. Major changes occur at 3150 cal a BP when Ericaceae and *Potamogeton* percentages increase, and at 2500 cal a BP when *Corylus avellana* percentages decrease.

LOI and the carbon (C) content of the sediments are high throughout the sequence (Fig. 3), with values ranging from ~31 to ~86% and ~27 to ~43%, respectively. LOI and C percentages correlate strongly, decreasing during the Subboreal zone compared to the Atlantic, and increasing from the Subatlantic onwards. Nitrogen (N) values also show a slight

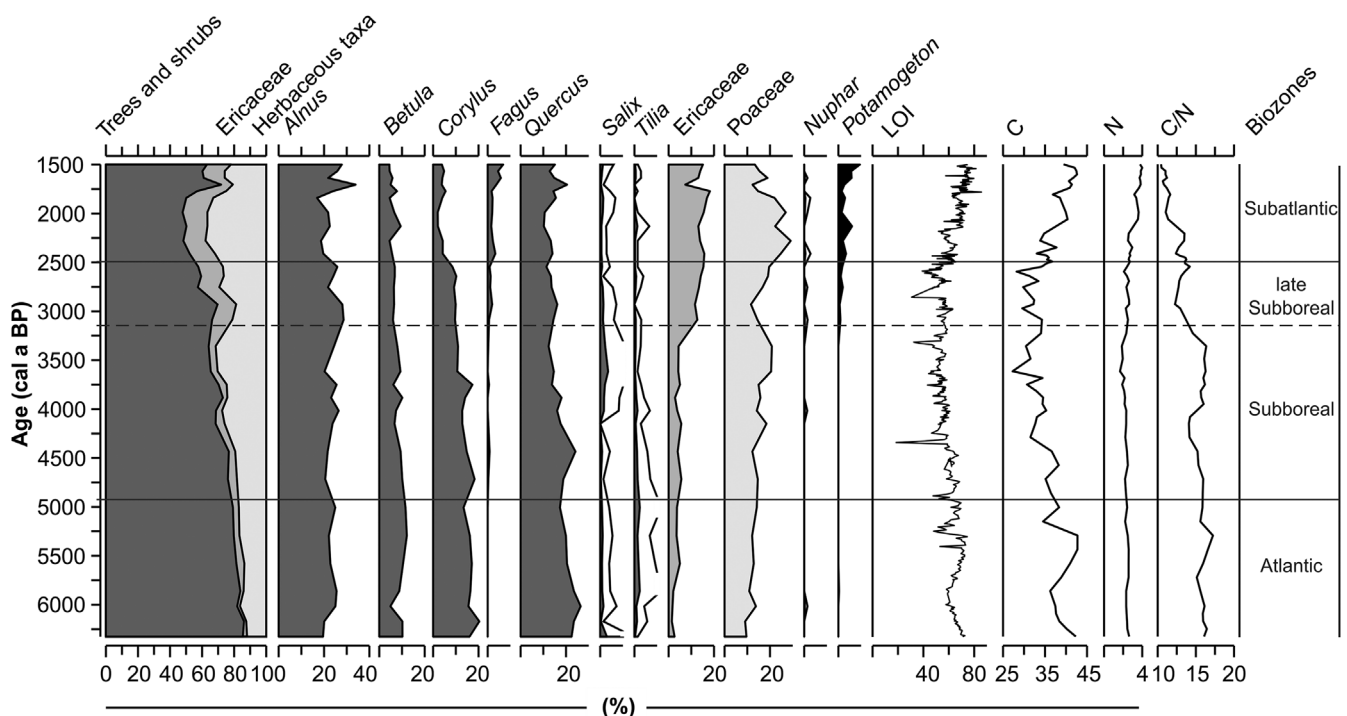


Figure 3. Microfossil diagram [main diagram and selected taxa (%)] and soil chemical parameters (loss-on-ignition, carbon content, nitrogen content and C/N ratio) for Uddelermeer core UDD-E. All data are expressed as percentages, except for the C/N ratio. Zonation was determined by Engels *et al.* (2016).

increase during the Subatlantic. The C/N ratio is high throughout the Atlantic and Subboreal zones (values > 15), but decreases strongly from the start of the late-Subboreal to values close to 10 in the Subatlantic. The decrease in C/N values coincides with the decrease in Poaceae pollen percentages and increase in Ericaceae percentages at the start of the late Subboreal (~ 3150 cal a BP).

n-Alkane concentrations

The total concentration of *n*-alkanes is high throughout the sequence, and varies between 329 and $1317 \mu\text{g g}^{-1}\text{C}$ (Fig. 4). The carbon preference index is > 5 , indicating that degradation rates were low and that the *n*-alkanes are well preserved in the sediments (Allan and Douglas, 1977). The concentration records of the individual homologues show that the C_{23} *n*-alkane concentration is fairly constant through time, with a slightly higher abundance at the onset of the record. C_{25} , C_{27} and C_{29} show largely consistent changes, with high abundances at the start of the record (Fig. 4), and a decrease in concentration during the Atlantic zone. Their concentrations increase during the Subboreal zone and drop suddenly at the start of the late Subboreal, after which the concentrations continue to decrease towards the top of the record. Homologues C_{31} and C_{33} show low abundances in the Atlantic, increase during the Subboreal and rise sharply at the Subboreal–Subatlantic transition. During the Subatlantic zone, their concentrations decrease along with the total sum of *n*-alkanes. The changes in relative concentrations of the *n*-alkane homologues are summarized in the $\text{C}_{27}/\text{C}_{31}$ ratio (Fig. 4). The values of the $\text{C}_{27}/\text{C}_{31}$ ratio lie between 0.4 and 3.1, starting with high values at the start of the Atlantic, and decreasing to around 1 in the Subboreal zone. The ratio drops below 1 and remains stable at low values throughout the remainder of the record at the onset of the late Subboreal zone.

Plant wax hydrogen-isotope ratios

The δD values of the odd-numbered *n*-alkanes C_{23} to C_{31} could be measured throughout the core (except for C_{23} in five samples; Fig. 5). The hydrogen isotope composition of the

other homologues ($< \text{C}_{23}$ and $> \text{C}_{31}$) could not be determined as their concentration in the samples was too low. The depth profile of δD reconstructed from C_{23} is most variable through time.

Each homologue shows a slightly different trend during the Atlantic biozone: *n*-alkanes C_{27} , C_{29} and C_{31} display a period of increased values between ~ 5600 and ~ 5000 cal a BP, each with a different amplitude. Homologue C_{25} shows gradually declining values, while C_{31} is relatively enriched (ca. -175‰) in the deepest part of the core ($6330\text{--}6000$ cal a BP).

The *n*-alkanes C_{25} , C_{27} , C_{29} and C_{31} show largely the same trend in δD values from the Subboreal zone onward: decreased values during the Subboreal until ~ 3500 cal a BP (averages of all Subboreal samples: -180 , -177 , -185 and -187‰ per homologue, respectively), when they increase gradually to higher values during the late Subboreal and Subatlantic (averages: -167 , -172 , -180 and -184‰ , respectively). This amounts to shifts in δD values between 3500 and 3150 cal a BP of 13 , 5 , 5 and 3‰ , respectively (first three values are higher than twice the mean standard deviation of all sample values calculated at 1.64‰). From 3150 cal a BP onwards, δD values appear to be stable for all homologues.

BrGDGTs

The ratio of the branched and isoprenoid tetraether (BIT) record for Uddelermeer shows values that are consistently close to 1, although they decrease slightly to 0.97 at ~ 3150 BP (Fig. 6A). BrGDGT concentrations vary between ~ 20 and $150 \mu\text{g g C}^{-1}$, and are highest during the Atlantic, start of the Subboreal and Subatlantic biozones. The isomer ratio of pentamethylated brGDGTs [IR_{penta} : 6-methyl/(5-methyl + 6-methyl) of all pentamethylated brGDGTs] is generally low, but increases from ~ 0.16 to ~ 0.21 at the Subboreal to late Subboreal transition at 3150 cal a BP. Due to the lack of a lake-specific transfer function based on brGDGT analysis with the new HPLC method with improved chromatography, MATs are based on the latest soil calibration of De Jonge *et al.* (2014a). Therefore, the temperature record should primarily be used to identify trends and relative changes, rather than absolute changes. The error associated with the

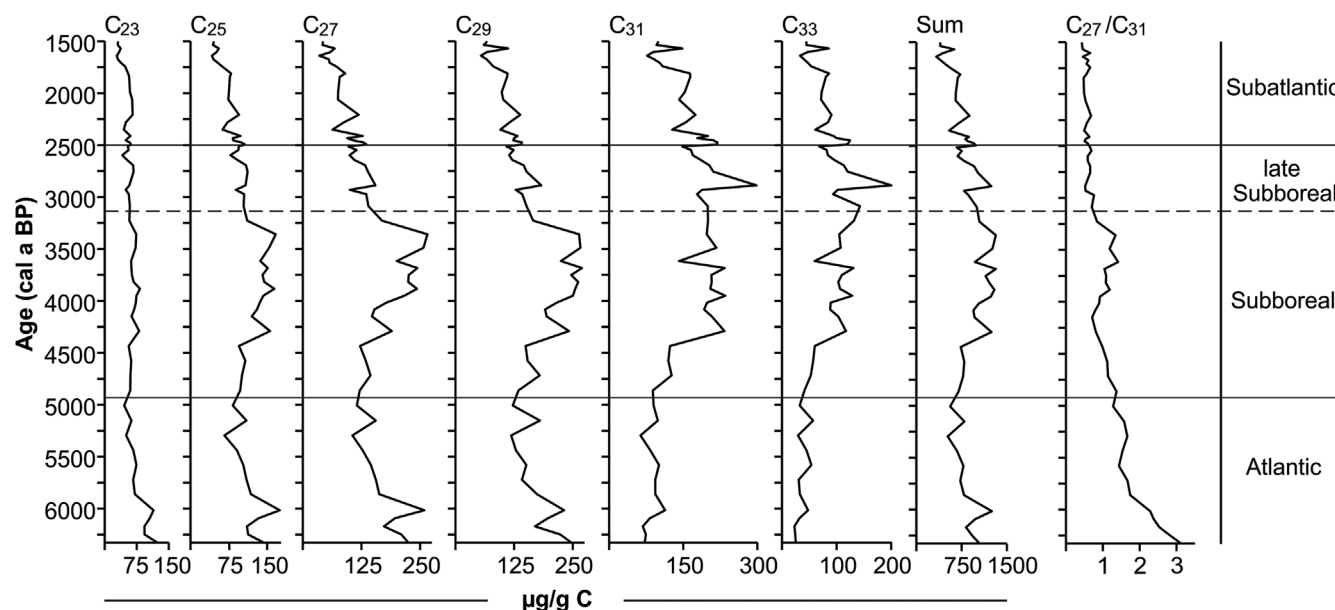


Figure 4. *n*-Alkane abundances for Uddelermeer core UDD-E. The figure shows the odd C_{23} to C_{33} homologues separately, the sum of all *n*-alkane homologues (Sum), and the ratio of C_{27} to C_{31} . All variables except the $\text{C}_{27}/\text{C}_{31}$ ratio are expressed as $\mu\text{g g}^{-1}\text{C}$. The right-hand side column shows the biozones as derived from palynological analyses (Fig. 3). Note the different x-axes used for each graph.

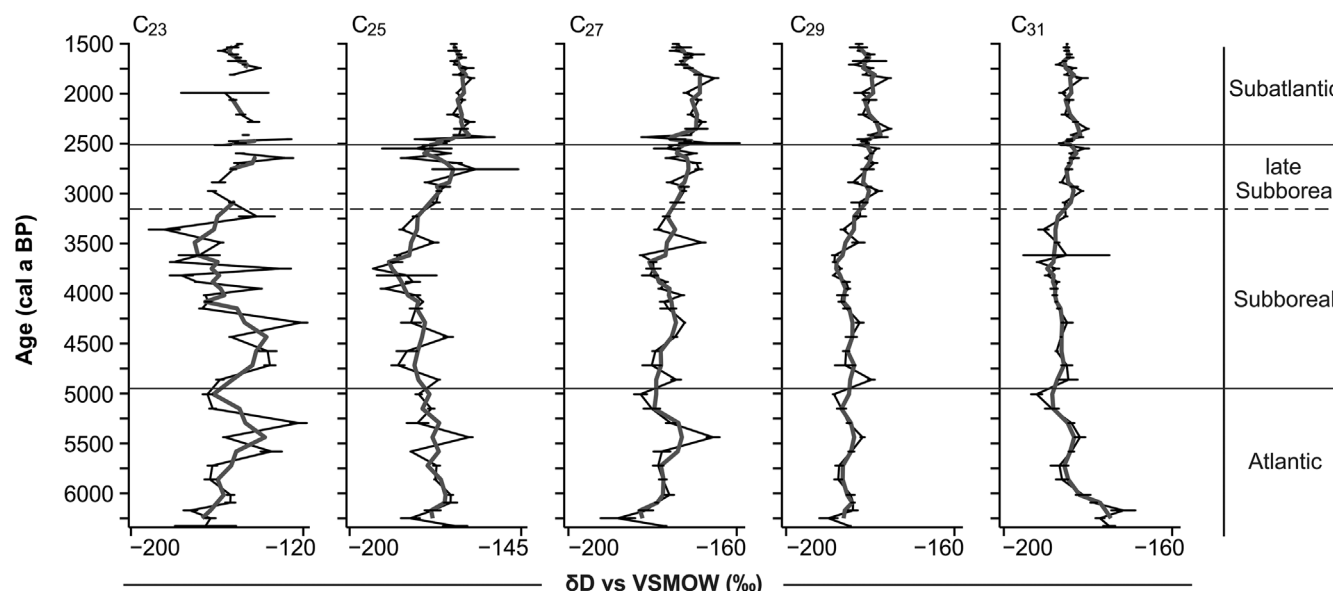


Figure 5. Hydrogen isotopic ratios of five *n*-alkanes with high concentrations in the sedimentary samples. Averages of three replicate measurements of each sample are plotted with their standard deviations. Grey lines represent the moving averages over three samples. Zonation as derived from palynological analyses (Fig. 3). Note the different x-axes used for each graph.

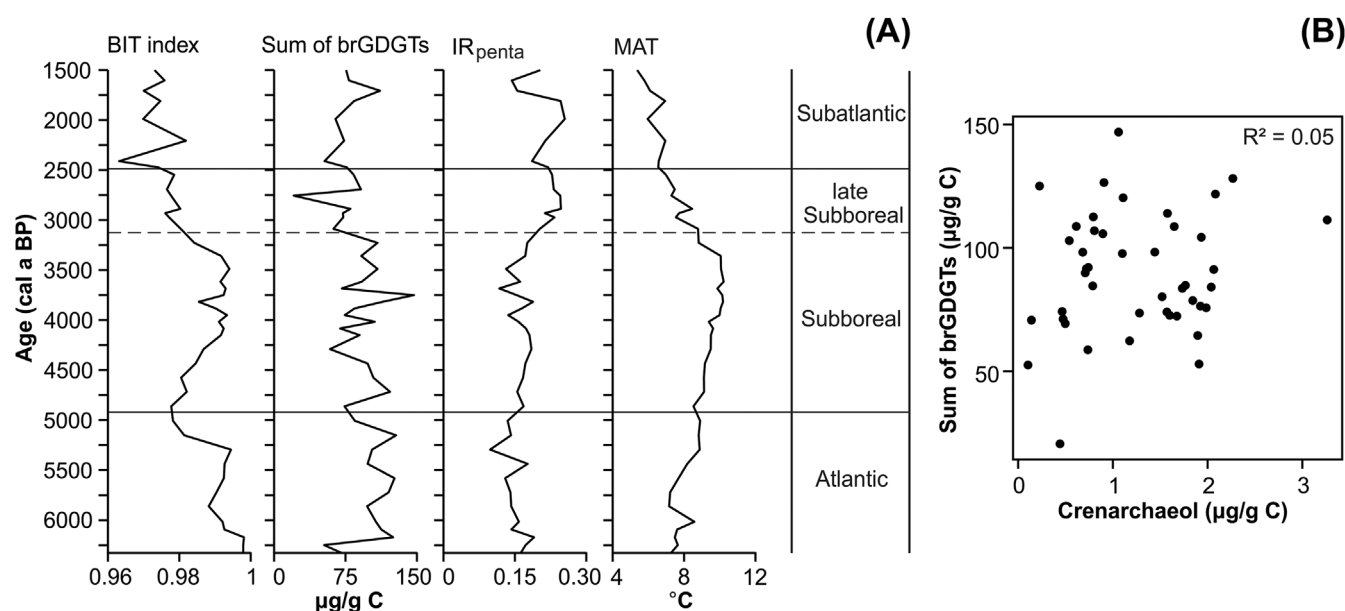


Figure 6. (A) BrGDGT data. From left to right: BIT index, sum of brGDGTs ($\mu\text{g g}^{-1}\text{C}$), isomer ratio (IR_{penta}) and MAT ($^{\circ}\text{C}$). Zonation as derived from palynological analyses (Fig. 3). (B) Correlation between the concentration of crenarchaeol and the sum of all brGDGTs.

soil calibration is 4.6°C (De Jonge *et al.*, 2014a). However, this uncertainty is probably caused by the heterogeneity of soils in the global calibration dataset and accompanying variation in environmental parameters, and can be considered largely systematic. By applying the calibration to one location, as in our case, this systematic error should be much smaller, although unfortunately difficult to constrain. Reconstructed MATs reflect a cooling from 10 to 6°C at 3150 cal a BP.

Discussion

Comparison of independent vegetation-derived palaeoenvironment proxies

Sedimentary *n*-alkane record

Although each species has a specific distribution of *n*-alkane chains (Fig. 2), interpretation of their signal in a lake sedimentary record is not straightforward as the alkane

distribution in a lake sediment sample is composed of a mix of *n*-alkane homologues derived from different species at different ratios. Therefore, shifts in vegetation are usually expressed in changes of the ratios of certain *n*-alkane homologues (e.g. Ishiwatari *et al.*, 2005; Jansen *et al.*, 2008). Commonly applied ratios use C_{31} as an indicator for grass species (Maffei, 1996) and C_{27} or C_{29} for woody species (Cranwell, 1973; Jansen *et al.*, 2006; D'Anjou *et al.*, 2012; Zech *et al.*, 2012). However, care must be taken when applying such ratios to a specific study site, as they are based on data from a large range of sites with different climates and ecosystems. Extrapolation can be erroneous because chain length patterns of modern plants can show substantial spatial variation (Zhang *et al.*, 2004; Kirkels *et al.*, 2013). The source of a certain *n*-alkane homologue may also be different between sites. For example, *n*-alkanes of mid-chain length (C_{23} and C_{25}) are proposed to derive mainly from non-emergent aquatic plant species in lakes (Ficken *et al.*, 2000),

but from *Sphagnum* species in peat bogs (Nott *et al.*, 2000). Lake Uddelermeer presently does not contain high abundances of aquatic plants; the only aquatic species observed during coring was *Nuphar lutea*, which produces low amounts of *n*-alkanes in general and no C_{23} . *Betula pendula* growing around the lake produces medium to high concentrations of C_{23} and C_{25} *n*-alkanes (Fig. 2).

The C_{27}/C_{31} ratio of the Uddelermeer record captures the variation of *n*-alkanes throughout the core very well (Fig. 4). However, the C_{27}/C_{31} ratio may not be indicative for woody versus grass species at this site. Instead, the C_{31} alkane in the Uddelermeer sediments probably derives from *Calluna vulgaris*, as this plant species shows high C_{31} concentrations ($>125 \mu\text{g g}^{-1}$ dry leaf material; Fig. 2) in the modern plant measurements. Furthermore, of the grass species, *Phragmites australis* (reed) is expected to contribute the most biomass to the lake sediments, but it does not produce the C_{31} homologue (Fig. 2). The C_{27} homologue is probably derived from tree species *Alnus glutinosa* and *Salix cinerea*, both common around lakes. Therefore, the C_{27}/C_{31} ratio is likely to be an indicator of closed (i.e. trees) versus open (i.e. heath) vegetation around Lake Uddelermeer, and thus reflects an expansion of the heathlands around the lake.

A commonly used representation of *n*-alkane records is the average chain length (ACL). However, as the C_{27}/C_{31} ratio in this case shows the same trend as the ACL curve, and as it is difficult to attribute changes in ACL to specific vegetation changes, we will focus on the C_{27}/C_{31} ratio for our vegetation reconstruction.

Local versus regional vegetation signals

The C_{27}/C_{31} ratio shows a gradual decrease from 6330 to ~ 4000 cal a BP and a relatively abrupt decrease at 3150 cal a BP, indicating that the vegetation around the lake became more open through time (Fig. 7). The decrease in C_{27}/C_{31} values at ~ 3150 cal a BP is driven by a sudden drop in C_{27}

alkane concentrations. The pollen diagram shows a similar but less obvious trend towards more openness through time, with declining arboreal pollen percentages (Fig. 3). This increased openness is probably the effect of increased human influence in the area. *Alnus* and *Salix* are relatively constant throughout the sequence, while *Corylus avellana* starts to decrease significantly after 2500 cal a BP (Subboreal–Subatlantic transition). Ericaceae pollen percentages increase at 3150 cal a BP, but the C_{31} *n*-alkane homologue (expected to be mainly produced by heath) does not follow the trend of the Ericaceae pollen curve. The discrepancy between the plant wax and pollen data is probably caused by the differences in source area of the two vegetation proxies. Pollen has its source in local, extra-local and regional vegetation (Faegri and Iversen, 1989; Olivera *et al.*, 2009), whereas plant waxes are thought to mainly represent *in situ* plants and plants growing on the lakeshore (Rao *et al.*, 2011; Jansen *et al.*, 2013), and should thus reflect the macrophyte vegetation and vegetation around the borders of the lake. Aerosol transportation is considered negligible compared to the high biomass input into the lake. Alternatively, a possible cause of the discrepancy between plant wax and pollen data is the source of plant waxes, which is confined to a limited number of plant species that dominate the *n*-alkane input into the sediments, e.g. certain tree species (Fig. 2). If these tree species are present around the lake throughout the sequence, changes in other species could be overshadowed. This might be the case with *Potamogeton*, which has been shown to produce mainly mid-chain-length *n*-alkanes (e.g. Aichner *et al.*, 2010). Where *Potamogeton* pollen increases from 3150 cal a BP, the C_{25} concentration declines and C_{23} remains unchanged. The contribution of *Potamogeton* to deposited mid-chain-length *n*-alkanes may be insignificant compared to the contribution of, for example, *Betula pendula*.

From the combined interpretation of the two vegetation proxies (*n*-alkanes and pollen) we can infer that at around 3150 cal a BP the lakeshore and area directly surrounding

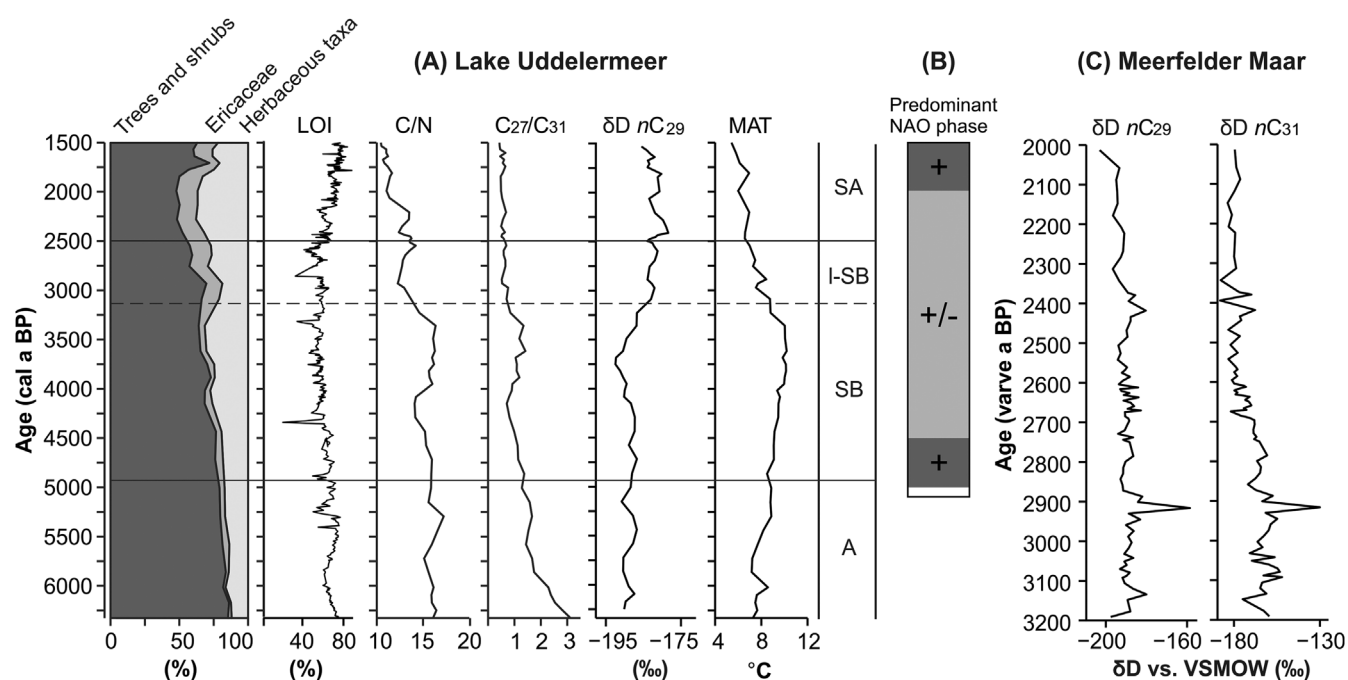


Figure 7. (A) Summary figure of proxy records from Uddelermeer (A). Uddelermeer records from left to right: main pollen diagram (%), LOI (%), C/N ratio, C_{27}/C_{31} *n*-alkane ratio, moving average of δD ratio of *n*-alkane C_{29} (δD vs. VSMOW in ‰) and brGDGT-derived MAT (°C). Zonation as derived from palynological analyses (Fig. 3). (B) Expected NAO phase as reconstructed by Olsen *et al.* (2012) on the time scale of Lake Uddelermeer; either predominantly positive or intermittently negative. (C) δD record of Meerfelder Maar, showing the δD ratio of *n*-alkanes C_{29} and C_{31} (δD vs. VSMOW in ‰).

Uddelermeer became more open, as shown by the decrease in *n*-alkane input from tree leaves. Heathland expands regionally at this time, as inferred from the pollen spectrum. Decreasing *Corylus avellana* pollen percentages suggest that a regional vegetation change occurs at 2500 cal a BP, consistent with a transition to wetter and cooler climate conditions (van Geel *et al.*, 1996). The vegetation around the lake does not seem to have been affected at this time, as concentrations of sedimentary *n*-alkanes remain stable in this part of the record. However, when the *n*-alkane record seems stable, species that do not contribute much to the *n*-alkane signal might still have changed in abundance. Additionally, different species with the same *n*-alkane signature (such as *Alnus glutinosa* and *Salix cinerea*) could theoretically replace each other without a signal showing up in the sedimentary record.

The combined interpretation of the proxies shows that biomarkers and pollen can be used to construct a robust and comprehensive picture of changing vegetation through time, especially when considering regional versus *in situ* vegetation change.

Environmental change at Lake Uddelermeer around 3150 cal a BP

Temperature

The temperature record derived from changes in brGDGT distributions throughout the sediments of Uddelermeer indicates that MAT was 10 °C during the Subboreal biozone, decreasing to about 6 °C in the Subatlantic biozone (Fig. 6A). This change is larger than expected. Quantitative temperature reconstruction based on brGDGTs in lakes may be complicated by mixed sources of brGDGTs archived in lacustrine sediments (Tierney and Russell, 2009). As well as in soils, brGDGTs may also be produced in the water column or in the lake sediment (e.g. Tierney and Russell, 2009; Loomis *et al.*, 2011), which may overprint the soil brGDGT signature delivered to the lake. Indeed, *in situ*, aquatic contribution has previously resulted in substantial underestimations of reconstructed MAT values upon application of brGDGT-based palaeothermometry on lake sediments (e.g. Zink *et al.*, 2010; Blaga *et al.*, 2010; Tierney *et al.*, 2010).

In the Uddelermeer sedimentary archive, BIT index values are consistently high (>0.96, Fig. 6A). As the BIT ratio is linked to the relative input of soil material to the lake (where 1 indicates a soil-dominated signal; Hopmans *et al.*, 2004), the high values suggest that aquatic contribution is limited in Uddelermeer. The fact that the concentration of crenarchaeol, the aquatic end-member of the BIT index (Hopmans *et al.*, 2004), and the sum of all brGDGTs do not correlate indicates that they have different sources (Fig. 6B). Additionally, the IR_{penta}, which indicates the relative contribution of 6-methyl brGDGTs, is low throughout the record (0.10–0.26; Fig. 6A), whereas high IR values have been reported for aquatic environments so far (>0.5; De Jonge *et al.*, 2014b; Sinninghe Damsté, 2016). The IR shows a positive relationship to pH in soils (De Jonge *et al.*, 2014a), and the relatively high IR values found in the aquatic environment have subsequently been attributed to the generally higher pH of an aquatic system (e.g. De Jonge *et al.*, 2014b). The slight increase in IR_{penta} from 3150 cal a BP onwards (from 0.16 to 0.21) may thus indicate either a decline in soil input caused by decreased erosion and subsequent decreased runoff, or a slight increase in primary production in the lake, although the range of this change is marginal compared to the range of values in the global soil calibration set (0–1.0; De Jonge *et al.*, 2014a).

Nevertheless, this trend is supported by a simultaneous, albeit minor decrease in BIT index values (from 0.99 to 0.98), as well as in the C/N ratio of the lake sediment (Fig. 3). The decreasing C/N ratio values at 3150 cal a BP indicate that either terrestrial organic matter input decreased or primary production in the lake increased (Kaushal & Binford, 1999). Alternatively, the increase in IR_{penta} may reflect a change in environmental conditions, such as an increase in soil pH due to drier conditions. An addition of *in situ* produced brGDGTs from 3150 cal a BP onwards may explain the larger than expected temperature drop observed around this time.

Hydrology

The δD signal derived from plant waxes is thought to reflect the hydrogen-isotopic composition of plant leaf water and by extension precipitation, and can therefore be used to reconstruct hydrological changes through time (Sachse *et al.*, 2012; Kahmen *et al.*, 2013). The δD value of precipitation in temperate regions is mainly determined by air temperature (a decrease in temperature leads to a lower deuterium content of precipitation) and moisture source region (changing the transport distance of the air mass or the temperature of the moisture source of clouds; Sachse *et al.*, 2012).

However, interpretation of δD values of plant waxes is not unambiguous as is shown by the differences in δD values between the individual *n*-alkane homologues (Fig. 5). These variations may be due to different source organisms for each homologue (Sachse *et al.*, 2012). Additionally, the dominant source for each chain may change through time. Part of the differences in δD values between source organisms – and thus *n*-alkane homologues – can be caused by different sources of growth water. For instance, the δD values of *n*-alkane homologues produced by aquatic plant species track the δD values of the lake water (Guenther *et al.*, 2013) and are not affected by evapotranspirative D enrichment as terrestrial plants are. The main *n*-alkane homologue thought to derive from aquatic plants is C₂₃. The C₂₃ *n*-alkane shows a δD signal different from the other homologues in the Uddelermeer sediments and is most variable through time. However, the major source of C₂₃ in Uddelermeer may be *Betula pendula*, as indicated by the high concentrations of C₂₃ in its modern leaf material (Fig. 2) and its high abundance in the pollen assemblages (Fig. 3). Alternatively, C₂₃ may derive from a mixture of terrestrial and aquatic sources.

The comparison of several vegetation-derived proxy records enables us to identify changes in δD trends caused by vegetation change and to separate these from changes caused by climate. The change from relatively high δD values of C₃₁ in the deepest part of the record (6330–6000 cal a BP) to lower values thereafter may be the result of a change in vegetation around the lake rather than a change in climate, as a decrease in the C₂₇/C₃₁ ratio around this time indicates a change in local vegetation. The most consistent δD change in the core sequence starts at 3500 cal a BP, pre-dating the vegetation change at 3150 cal a BP. We interpret the δD increase at 3500 cal a BP as a climate signal, as the shift is present in four out of five *n*-alkane homologues and precedes the vegetation change by 350 years.

Late Holocene atmospheric circulation change in north-west Europe

All Uddelermeer proxy records show strong changes at 3150 cal a BP, when changes in the concentrations of individual *n*-alkanes indicate an opening of the local vegetation,

and brGDGTs and the decreasing C/N ratio indicate that the nature and source of organic matter input into the lake changed towards a larger contribution of aquatically produced matter. In addition, Engels *et al.* (2016) used a combination of ground-penetrating radar imagery, palaeoecology and sedimentology to reconstruct a decrease in lake levels to levels ~ 2.5 m lower than at present at 3150 cal a BP.

All these changes closely follow a shift to higher values in our compound-specific δD records at 3500 cal a BP. This increase could be explained by three different mechanisms: (i) an increase in air temperature, (ii) an increase in evapotranspiration or (iii) a change in moisture source region. Although an increase in temperature or evapotranspiration could also explain the lower lake levels during the late Subboreal at Uddelermeer, the brGDGT-based MAT record indicates a trend towards cooler conditions. Furthermore, none of the records currently available for north-west Europe provide evidence for the occurrence of either increased temperature or evapotranspiration during this period. For instance, most peat bogs in north-west Europe show a shift to wetter conditions at the 2.8-kyr climate event and the Subboreal–Subatlantic transition, with no evidence for a preceding dry period (van Geel *et al.*, 1996, 2014; Engels and van Geel, 2012). The exception is a raised bog in north-west Ireland, where drier conditions around 2800 cal a BP preceded a subsequent shift to wetter conditions (Plunkett and Swindles, 2008). The delay in response might be due to local variability of the raised bog (e.g. hummocks are thought to be less responsive than hollows; Blaauw *et al.*, 2004), but Plunkett and Swindles (2008) suggest that the non-uniform response to the 2.8-kyr event in European records might be due to high spatial complexity in the effect of changing atmospheric circulation.

The dominant mode of variability of atmospheric circulation in the present-day climate in western Europe is the NAO (Olsen *et al.*, 2012). The NAO index is calculated from the difference in atmospheric pressure between the Icelandic low and the Azores high, and controls the strength and direction of the westerly winds and storm tracks across the North Atlantic. NAO influences both temperature and precipitation patterns, and influences oceanic circulation and Arctic sea ice distribution as well (e.g. Strong *et al.*, 2009). When the index is positive, northern Europe and the eastern US tend to be mild and wet, while Greenland and northern Canada display cold and dry conditions. A strong NAO control was found in the instrumental record of $\delta^{18}O$ values of precipitation in Europe, especially during the winter months (Field, 2010). The mean $\delta^{18}O$ of precipitation appears to be higher during positive NAO phases (consistent with higher temperatures and increased precipitation; Baldini *et al.*, 2008; Field, 2010; Langebroek *et al.*, 2011). This effect is most pronounced in central western Europe (Langebroek *et al.*, 2011), where higher $\delta^{18}O$ values in the instrumental record were associated with a northward shift in the storm track and increasing south-westerly flow (Field, 2010). Western sites have a general tendency towards higher values, being marine-influenced (Langebroek *et al.*, 2011). As δD in meteoric water is linearly related to $\delta^{18}O$ (Craig, 1961), δD would be similarly affected by NAO phase.

As the instrumental record shows a strong relationship between NAO phase and $\delta^{18}O$, it should be possible to identify large-scale changes in NAO phases in past records of the isotopic composition of precipitation (Langebroek *et al.*, 2011). The increase in δD values in our record

would suggest a shift to more positive NAO from 3500 cal a BP onwards, which is in line with increased precipitation identified at nearby peat bogs (Engbertsdijkveen, Fig. 1A; van Geel *et al.*, 1996). However, Rach *et al.* (2017) report a long-term trend of decreasing δD values between 3200 and 2000 varve a BP at nearby Meerfelder Maar (Figs 1A and 7), consistent with atmospheric conditions resembling negative NAO conditions.

Olsen *et al.* (2012) provide a record of past NAO phases reconstructed from a combination of records. They show that the NAO changed from mostly positive between 5000 and 4500 cal a BP to variable, intermittently negative conditions between 4500 and 2000 cal a BP (Fig. 7). Similarly, Martin-Puertas *et al.* (2012) modelled sea-level pressure during the Homeric minimum and argue that atmospheric conditions resembling a negative NAO phase prevailed during this period. A negative NAO phase is in line with the decreasing δD values at Meerfelder Maar, suggesting that the NAO signal was overprinted by other factors at Lake Uddelermeer. This is corroborated by the results of Baldini *et al.* (2008), who show that in the instrumental record, the link between $\delta^{18}O$ and NAO is stronger at sites close to Meerfelder Maar (such as Wasserkuppe Rhoen and Koblenz) than at the more north-western sites closer to Uddelermeer (such as Emmerich; see also Supporting Information Fig. S1 in Appendix S2). Baldini *et al.* (2008) further explain that the impact of the NAO index on $\delta^{18}O$ in central Europe is caused by the higher frequency of cold easterly winds carrying isotopically depleted precipitation during negative NAO phases. As Uddelermeer lies in a more maritime area than Meerfelder Maar, it might be influenced more by warmer westerly winds carrying ^{18}O - and D-enriched precipitation from the North Atlantic, prevailing even during negative NAO. Alternatively, the increase in δD values at Lake Uddelermeer was caused by a change in moisture source unrelated to NAO, while the decline in δD values at Meerfelder Maar was caused by increased humidity. This would be in line with increased humidity at the Subboreal–Subatlantic transition inferred from terrestrial records in north-west Europe (van Geel *et al.*, 2014).

Although changing atmospheric circulation (whether related to NAO phases or not) may explain the increase in δD values at Lake Uddelermeer, the change pre-dates the 2.8-kyr climate event by ~ 700 years. This is in line with the review of ~ 50 palaeoclimatic records from across the globe that showed complex changes in climate occur between 3500 and 2500 cal a BP (Mayewski *et al.*, 2004). Apart from the different nature of responses to the 2.8-kyr event, it is also possible that the timing of responses is variable. Alternatively, different sensitivities of the δD of leaf waxes and other proxies used to define the 2.8-kyr event may be responsible for this apparent delay.

Conclusions

We applied a combination of molecular palaeoecological techniques to a sediment core from Lake Uddelermeer spanning part of the middle and late Holocene (6300–1500 cal a BP), and compared our results to existing palynological data to reconstruct changes in vegetation and atmospheric circulation patterns around the 2.8-kyr event.

Firstly, a comparison of plant wax distributions in sediment samples to those in modern plant material collected from the vicinity of Lake Uddelermeer reveals a change in the local vegetation from tree-dominated (*Alnus* and *Salix*) to open heathland at ~ 3150 cal a BP. Palynological data show a

similar, but less obvious trend, towards more open vegetation in the area, supporting the use of *n*-alkanes as an additional proxy for past vegetation changes. brGDGT-derived MAT reconstruction indicates a cooling trend coinciding with the opening of the landscape around the lake. Furthermore, brGDGT distributions and the C/N ratio indicate a change in organic matter source around 3150 BP, possibly related to a decreased input of terrestrial biomass into the lake, increased productivity in the water column and/or a lowering of lake levels.

Secondly, the δD values of most *n*-alkanes show an increase at 3500 cal a BP (range of change 3–15‰), which may have been caused by an increase in air temperature, an increase in evapotranspiration or a change in moisture source region/pathway. An increase in air temperature is unlikely, as indicated by the brGDGT record. Increases in evapotranspiration are not in line with increased humidity in most of the records of north-west Europe. We therefore argue that a change in moisture source pathway caused by a change in atmospheric circulation is the most likely driver of the changes we observe in our δD record. Plant wax δD values from Lake Meerfelder Maar in western Germany show a trend that is opposite to that in the Lake Uddelermeer sediments between 3200 and 2000 cal a BP, possibly caused by a situation resembling a negative NOA phase. Confounding factors related to the more maritime position of Uddelermeer could cause the opposite shift observed there. Alternatively, δD values at Meerfelder Maar might be mostly affected by increased humidity (decreased evapotranspiration), while at Uddelermeer a change in atmospheric circulation (unrelated to NAO) was a stronger driver. A non-uniform response to atmospheric circulation change may also explain the different timing of the event, causing the changes at Uddelermeer to occur at 3500 and 3150 cal a BP as opposed to 2800 cal a BP.

This study shows the importance of combining well-understood traditional proxies and novel techniques to deduce a robust and complete picture of vegetation change, and a better understanding of the mechanisms underlying climate change in the Holocene.

Supporting Information

Appendix S1. Extended description of the methods used for biomarker analysis.

Appendix S2. GNIP data for The Netherlands and Germany.

Figure S1. Mean $\delta^{18}O$ values of precipitation for the period 1980–2000 from the Global Network of Isotopes in Precipitation database.

Acknowledgements. We thank the following people for their contribution to this study: Wim Z. Hoek and Andy Lotter for logistical support; Nelleke van Asch, Erik J. de Boer, Remko Engels, Tom Peters, Julia Sassi, Marchien Wolma, Tim Winkels and Hessel Woolderink for help during fieldwork; Joke W. Westerveld, Leo Hoitinga and Rick Helmus for help with lipid biomarker preparation; Bernd Hoffmann for help with deuterium measurements; Oliver Rach for discussion of the Meerfelder Maar data; Bas van Geel for invaluable feedback on an earlier version of the manuscript; Elliot Swallow for feedback on English spelling, grammar and syntax; and the two anonymous reviewers for their constructive comments. Tieke Poelen and Kroondomein het Loo are thanked for granting permission to access the site. The research of S.E. and F.P. is financed by the Netherlands Organization for Scientific Research (NWO, project 863.11.009 and 863.13.016, respectively). NWO grant 834.11.006 enabled the purchase of the UHPLC-MS system used for GDGT analyses. We dedicate this paper to the memory of our much-missed

colleague and friend Sjoerd Bohncke, who passed away during the preparation of this manuscript.

Abbreviations. ACL, average chain length; BIT, branched and isoprenoid tetraether; brGDGT, branched glycerol dialkyl glycerol tetraether; GC/MS, gas chromatography-mass spectrometry; IRMS, isotope ratio mass spectrometer; LOI, loss-on-ignition; MAT, mean air temperature; NAO, North Atlantic Oscillation; VSMOW, Vienna Standard Mean Ocean water.

References

- Aichner B, Herzsich U, Wilkes H *et al.* 2010. δD values of *n*-alkanes in Tibetan lake sediments and aquatic macrophytes – A surface sediment study and application to a 16 ka record from Lake Koucha. *Organic Geochemistry* **41**: 779–790.
- Allan J, Douglas AG. 1977. Variations in the content and distribution of *n*-alkanes in a series of carboniferous vitrinites and sporinites of bituminous rank. *Geochimica et Cosmochimica Acta* **41**: 1223–1230.
- Baldini LM, McDermott F, Foley AM *et al.* 2008. Spatial variability in the European winter precipitation $\delta^{18}O$ -NAO relationship: implications for reconstructing NAO-mode climate variability in the Holocene. *Geophysical Research Letters* **35**: L04709.
- Blaauw M, van Geel B, van der Plicht J. 2004. Solar forcing of climatic change during the mid-Holocene: indications from raised bogs in the Netherlands. *The Holocene* **14**: 35–44.
- Blaga CI, Reichart G-J, Schouten S *et al.* 2010. Branched glycerol dialkyl glycerol tetraethers in lake sediments: Can they be used as temperature and pH proxies? *Organic Geochemistry* **41**: 1225–1234.
- Bond G, Kromer B, Beer J *et al.* 2001. Persistent solar influence on North Atlantic climate during the Holocene. *Science* **294**: 2130–2136.
- Bond G, Showers W, Cheseby M *et al.* 1997. A pervasive millennial-scale cycle in North Atlantic Holocene and glacial climates. *Science* **278**: 1257–1266.
- Bronk Ramsey C. 2009. Bayesian analysis of radiocarbon dates. *Radiocarbon* **51**: 337–360.
- Charman DJ. 2010. Centennial climate variability in the British Isles during the mid-late Holocene. *Quaternary Science Reviews* **29**: 1539–1554.
- Charman DJ, Blundell A, Chiverrell RC *et al.* 2006. Compilation of non-annually resolved Holocene proxy climate records: stacked Holocene peatland palaeo-water table reconstructions from northern Britain. *Quaternary Science Reviews* **25**: 336–350.
- Craig H. 1961. Isotopic variations in meteoric waters. *Science* **133**: 1702–1703.
- Cranwell PA. 1973. Chain-length distribution of *n*-alkanes from lake sediments in relation to post-glacial environmental change. *Freshwater Biology* **3**: 259–265.
- Czymzik M, Muscheler R, Brauer A. 2016. Solar modulation of flood frequency in central Europe during spring and summer on interannual to multi-centennial timescales. *Climate of the Past* **12**: 799–805.
- D'Anjou RM, Bradley RS, Balascio NL *et al.* 2012. Climate impacts on human settlement and agricultural activities in northern Norway revealed through sediment biogeochemistry. *Proceedings of the National Academy of Sciences of the United States of America* **109**: 20332–20337.
- de Jonge C, Hopmans EC, Zell CI *et al.* 2014a. Occurrence and abundance of 6-methyl branched glycerol dialkyl glycerol tetraethers in soils: implications for palaeoclimate reconstruction. *Geochimica et Cosmochimica Acta* **141**: 97–112.
- de Jonge C, Stadnitskaia A, Hopmans EC *et al.* 2014b. In situ produced branched glycerol dialkyl glycerol tetraethers in suspended particulate matter from the Yenisei River, Eastern Siberia. *Geochimica et Cosmochimica Acta* **125**: 476–491.
- Eglinton TI, Eglinton G. 2008. Molecular proxies for paleoclimatology. *Earth and Planetary Science Letters* **275**: 1–16.
- Engels S, Bakker MAJ, Bohncke SJP *et al.* 2016. Centennial-scale lake-level lowstand at Lake Uddelermeer (The Netherlands) indicates changes in moisture source region prior to the 2.8-kyr event. *The Holocene* **26**: 1075–1091.
- Engels S, van Geel B. 2012. The effects of changing solar activity on climate: contributions from palaeoclimatological studies. *Journal of Space Weather and Space Climate* **2**: 1–9.

- Faegri K, Iversen J. 1989. *Textbook of Pollen Analysis*. John Wiley & Sons: Chichester, UK.
- Ficken KJ, Li B, Swain DL *et al.* 2000. An *n*-alkane proxy for the sedimentary input of submerged/floating freshwater aquatic macrophytes. *Organic Geochemistry* **31**: 745–749.
- Field RD. 2010. Observed and modeled controls on precipitation δ 18 O over Europe: From local temperature to the Northern Annular Mode. *Journal of Geophysical Research, Atmospheres* **115**: 1–14.
- Guenther F, Aichner B, Siegwolf R *et al.* 2013. A synthesis of hydrogen isotope variability and its hydrological significance at the Qinghai–Tibetan Plateau. *Quaternary International* **313–314**: 3–16.
- Haltia-Hovi E, Saarinen T, Kukkonen M. 2007. A 2000-year record of solar forcing on varved lake sediment in eastern Finland. *Quaternary Science Reviews* **26**: 678–689.
- Hopmans EC, Schouten S, Sinninghe Damsté JS. 2016. The effect of improved chromatography on GDGT-based palaeoproxies. *Organic Geochemistry* **93**: 1–6.
- Hopmans EC, Weijers JWH, Schefuß E *et al.* 2004. A novel proxy for terrestrial organic matter in sediments based on branched and isoprenoid tetraether lipids. *Earth and Planetary Science Letters* **224**: 107–116.
- Ishiwatari R, Yamamoto S, Uemura H. 2005. Lipid and lignin/cutin compounds in Lake Baikal sediments over the last 37 kyr: implications for glacial–interglacial palaeoenvironmental change. *Organic Geochemistry* **36**: 327–347.
- Jansen B, de Boer EJ, Cleef AM *et al.* 2013. Reconstruction of late Holocene forest dynamics in northern Ecuador from biomarkers and pollen in soil cores. *Palaeogeography, Palaeoclimatology, Palaeoecology* **386**: 607–619.
- Jansen B, Haussmann NS, Tonneijck FH *et al.* 2008. Characteristic straight-chain lipid ratios as a quick method to assess past forest–páramo transitions in the Ecuadorian Andes. *Palaeogeography, Palaeoclimatology, Palaeoecology* **262**: 129–139.
- Jansen B, Nierop KGJ, Hageman JA *et al.* 2006. The straight-chain lipid biomarker composition of plant species responsible for the dominant biomass production along two altitudinal transects in the Ecuadorian Andes. *Organic Geochemistry* **37**: 1514–1536.
- Juggins S. 2015. rioja: Analysis of Quaternary Science Data, R package version (0.9-9). Available at: <http://cran.r-project.org/package=rioja>.
- Kahmen A, Schefuß E, Sachse D. 2013. Leaf water deuterium enrichment shapes leaf wax *n*-alkane δ D values of angiosperm plants I: Experimental evidence and mechanistic insights. *Geochimica et Cosmochimica Acta* **111**: 39–49.
- Kaushal S, Binford MW. 1999. Relationship between C:N ratios of lake sediments, organic matter sources, and historical deforestation in Lake Pleasant, Massachusetts, USA. *Journal of Paleolimnology* **22**: 439–442.
- Kilian MR, van der Plicht J, van Geel B. 1995. Dating raised bogs: new aspects of AMS ^{14}C wiggle matching, a reservoir effect and climatic change. *Quaternary Science Reviews* **14**: 959–966.
- Kirkels FMSA, Jansen B, Kalbitz K. 2013. Consistency of plant-specific *n*-alkane patterns in pluggen ecosystems: a review. *The Holocene* **23**: 1355–1368.
- Langebroek PM, Werner M, Lohmann G. 2011. Climate information imprinted in oxygen-isotopic composition of precipitation in Europe. *Earth and Planetary Science Letters* **311**: 144–154.
- Loomis SE, Russell JM, Sinninghe Damsté JS. 2011. Distributions of branched GDGTs in soils and lake sediments from western Uganda: implications for a lacustrine paleothermometer. *Organic Geochemistry* **42**: 739–751.
- Maffei M. 1996. Chemotaxonomic significance of leaf wax alkanes in the Gramineae. *Biochemical Systematics and Ecology* **24**: 53–64.
- Magny M. 2004. Holocene climate variability as reflected by mid-European lake-level fluctuations and its probable impact on prehistoric human settlements. *Quaternary International* **113**: 65–79.
- Martin-Puertas C, Matthes K, Brauer A *et al.* 2012. Regional atmospheric circulation shifts induced by a grand solar minimum. *Nature Geoscience* **5**: 397–401.
- Mauquoy D, van Geel B, Blaauw M *et al.* 2002. Evidence from northwest European bogs shows ‘Little Ice Age’ climatic changes driven by variations in solar activity. *The Holocene* **12**: 1–6.
- Mayewski PA, Rohling EE, Curt Stager JC *et al.* 2004. Holocene climate variability. *Quaternary Research* **62**: 243–255.
- Nott CJ, Xie S, Avsejs LA *et al.* 2000. *n*-Alkane distributions in ombrotrophic mires as indicators of vegetation change related to climatic variation. *Organic Geochemistry* **31**: 231–235.
- Ojala AEK, Launonen I, Holmström L *et al.* 2015. Effects of solar forcing and North Atlantic oscillation on the climate of continental Scandinavia during the Holocene. *Quaternary Science Reviews* **112**: 153–171.
- Olivera MM, Duivenvoorden JF, Hooghiemstra H. 2009. Pollen rain and pollen representation across a forest–páramo ecotone in northern Ecuador. *Review of Palaeobotany and Palynology* **157**: 285–300.
- Olsen J, Anderson NJ, Knudsen MF. 2012. Variability of the North Atlantic Oscillation over the past 5,200 years. *Nature Geoscience* **5**: 808–812.
- Plunkett G, Swindles GT. 2008. Determining the sun’s influence on Lateglacial and Holocene climates: a focus on climate response to centennial-scale solar forcing at 2800 cal.BP. *Quaternary Science Reviews* **27**: 175–184.
- Polak B. 1959. A contribution to our knowledge of the vegetation and of the agriculture in the northern part of the Veluwe in prehistoric and early historic times. *Acta Botanica Neerlandica* **9**: 547–571.
- R Core Team. 2014. *R: A Language and Environment for Statistical Computing*. R Foundation for Statistical Computing: Vienna.
- Rach O, Engels S, Kahmen A *et al.* 2017. Hydrological and ecological changes in Western Europe between 3200 and 2000 years BP derived from lipid biomarker δ D values in Lake Meerfelder Maar sediments. *Quaternary Science Reviews*, **172**: 44–54.
- Rao ZG, Zhu ZY, Jia GD *et al.* 2011. Compound-specific hydrogen isotopes of long-chain *n*-alkanes extracted from topsoil under a grassland ecosystem in northern China. *Science China Earth Sciences* **54**: 1902–1911.
- Sachse D, Billault I, Bowen GJ *et al.* 2012. Molecular paleohydrology: interpreting the hydrogen-isotopic composition of lipid biomarkers from photosynthesizing organisms. *Annual Review of Earth and Planetary Sciences* **40**: 221–249.
- Sachse D, Radke J, Gleixner G. 2004. Hydrogen isotope ratios of recent lacustrine sedimentary *n*-alkanes record modern climate variability. *Geochimica et Cosmochimica Acta* **68**: 4877–4889.
- Sinninghe Damsté JS. 2016. Spatial heterogeneity of sources of branched tetraethers in shelf systems: the geochemistry of tetraethers in the Berau River delta (Kalimantan, Indonesia). *Geochimica et Cosmochimica Acta* **186**: 13–31.
- Strong C, Magnúsdóttir G, Stern H. 2009. Observed feedback between Winter Sea ice and the North Atlantic oscillation. *Journal of Climate* **22**: 6021–6032.
- Swindles GT, Lawson IT, Matthews IP *et al.* 2013. Centennial-scale climate change in Ireland during the Holocene. *Earth-Science Reviews* **126**: 300–320.
- Tierney JE, Russell JM. 2009. Distributions of branched GDGTs in a tropical lake system: implications for lacustrine application of the MBT/CBT paleoproxy. *Organic Geochemistry* **40**: 1032–1036.
- Tierney JE, Russell JM, Eggermont H *et al.* 2010. Environmental controls on branched tetraether lipid distributions in tropical East African lake sediments. *Geochimica et Cosmochimica Acta* **74**: 4902–4918.
- van Geel B. 1978. A palaeoecological study of Holocene peat bog sections in Germany and the Netherlands, based on the analysis of pollen, spores and macro- and microscopic remains of fungi, algae, cormophytes and animals. *Review of Palaeobotany and Palynology* **25**: 1–120.
- van Geel B, Buurman J, Waterbolk HT. 1996. Archaeological and palaeoecological indications of an abrupt climate change in The Netherlands, and evidence for climatological teleconnections around 2650 BP. *Journal of Quaternary Science* **11**: 451–460.
- van Geel B, Heijnis H, Charman DJ *et al.* 2014. Bog burst in the eastern Netherlands triggered by the 2.8 kyr BP climate event. *The Holocene* **24**: 1465–1477.
- Walker MJC, Berkelhammer M, Björck S *et al.* 2012. Formal subdivision of the Holocene Series/Epoch: a Discussion Paper by a Working Group of INTIMATE (Integration of ice-core, marine and terrestrial records) and the Subcommittee on Quaternary

- Stratigraphy (International Commission on Stratigraphy). *Journal of Quaternary Science* **27**: 649–659.
- Weijers JWH, Schouten S, van den Donker JC *et al.* 2007. Environmental controls on bacterial tetraether membrane lipid distribution in soils. *Geochimica et Cosmochimica Acta* **71**: 703–713.
- Wickham H. 2009. *ggplot2: Elegant Graphics for Data Analysis*. Springer: New York.
- Zech M, Rass S, Bugge B *et al.* 2012. Reconstruction of the late Quaternary paleoenvironments of the Nußloch loess paleosol sequence, Germany, using *n*-alkane biomarkers. *Quaternary Research* **78**: 226–235.
- Zhang Y, Togamura Y, Otsuki K. 2004. Study on the *n*-alkane patterns in some grasses and factors affecting the *n*-alkane patterns. *Journal of Agricultural Science* **142**: 469–475.
- Zink K-G, Vandergoes MJ, Mangelsdorf K *et al.* 2010. Application of bacterial glycerol dialkyl glycerol tetraethers (GDGTs) to develop modern and past temperature estimates from New Zealand lakes. *Organic Geochemistry* **41**: 1060–1066.